Surface Properties of Ice Studied by Atomic Force Microscopy

Astrid Döppenschmidt,* Michael Kappl, and Hans-Jürgen Butt

Institute of Physical Chemistry, Gutenberg University, 55099 Mainz, Germany

Received: March 5, 1998; In Final Form: July 13, 1998

The atomic force microscope was used to investigate surface properties of ice in a temperature range of −24 to −0.7 °C. An upper limit of the thickness of the liquidlike layer on the surface of ice was found to vary between about 12 nm at −24 °C and 70 nm at −0.7 °C. This was correlated with an increase of the adhesion force. In force-versus-distance measurements the tip penetrated the ice. This behavior can be interpreted in two ways: Either a "soft ice layer" exists between the liquidlike layer and bulk ice or the presence of the solid tip causes the ice surface to change its mechanical properties. Such an interfacial premelting might be relevant for friction. It might add to frictional heating as a cause for the lubricating liquid layer which reduces friction. In addition, friction was measured around −23 °C. With the atomic force microscope friction at individual microcontacts with a contact area of a few $(10\ \text{nm})^2$ can be determined. Friction increases with decreasing sliding velocity, which is probably due to the penetration of the tip into the ice at low velocities.

1. Introduction

The surface of ice plays an important role in physics, chemistry, and many technical applications. Winter sports such as skiing or skating, automobile traction, and ice breaker propulsion are some examples. The ice in polar stratospheric clouds is thought to accelerate the destruction of ozone in the stratosphere.[1−3] Since water is a unique solvent, the ice/water interface is important for biology and organic chemistry, for example for the microscopic study of macromolecules or polyelectrolytes.[4] Therefore the surface of ice has been the subject of several experimental investigations. Methods such as ellipsometry,[5−8] X-ray scattering,[9,10] proton channeling,[11] nuclear magnetic resonance (NMR),[12,13] scanning tunneling microscopy (STM),[14] and atomic force microscopy (AFM)[15−18] have been employed to examine its properties (for a review see refs 19 and 20).

Most authors agree that a liquidlike layer exists on the surface of ice. Liquid films change the adhesion and lubricating properties of surfaces and influence the reactivity of solids with gas molecules. The temperature range where this liquidlike layer exists, its thickness, and a theoretical explanation, however, are still under debate.[19,21−26]

Another partly unexplained phenomenon is the low friction on ice and snow.[27−33] The coefficient of friction is about 1 order of magnitude lower than on other solids. This is usually explained by a lubricating layer of water between the slider and ice. Reynolds thought that this layer of water is formed by high pressure.[34] However, later experiments proved that pressure induced melting is insignificant.[35−39] Nowadays it is generally accepted that friction induced heating is responsible for a melting of the ice surface.[27,30,31,36]

We used AFM[40] to study surface properties of ice. With AFM it is possible to determine an upper limit of the thickness of the liquidlike layer by measuring force-versus-distance curves. In addition, AFM was used to study friction. Friction experiments with AFM are motivated by the fact that contact between two sliding surfaces is limited to a small fraction of the apparent area. Only at certain points the two bodies are in contact, and only at these microcontacts friction occurs. Hence, to analyze friction, it is appropriate to study what happens at a single microcontact. This can be done with AFM. We used AFM to study velocity-dependent friction on ice at low velocities (0.2−60 μm/s) and with a microscopic interaction area of a few $(10\ \text{nm})^2$.

2. Experimental Methods

All measurements were done with a commercial AFM (NanoScope III, Multimode, Digital Instruments). We used two different kinds of V-shaped silicon nitride cantilevers. The cantilevers of Digital Instruments were 110 μm long and 0.6 μm thick. The tips had radii of curvature of about 25−60 nm.[41] We also used cantilevers from Olympus which were 100 μm long and 0.4 μm thick. They had radii of curvature of about 10 nm. Such a large variation in the radius of curvature makes a quantitative comparison of absolute forces between different tips difficult. Using Derjaguin's approximation, the absolute value of a force scales roughly with the radius of curvature.[42] However, results obtained with one tip under different conditions are quantitatively comparable. All cantilevers were gold coated on the backside. Spring constants, determined via measuring thermal fluctuations[43] as described in ref 44, were between 0.10 and 0.23 N/m with errors of 20%.

The deflection of the cantilever was determined by focusing the beam of a laser diode (initial power 1 mW, manufacturer specification) onto the back of the cantilever. The intensity of the laser beam was reduced by an optical filter by a factor of 0.1 in order to avoid significant heating of the tip. The position of the reflected beam was measured with a segmented photodiode. The cantilever was tilted by roughly 7° with respect to the sample surface.

To obtain force-versus-distance curves, the original deflection-versus-position curves had to be converted by $d = d_{\text{piezo}} - d_{\text{def}}/m_{\text{cl}}$. d is the distance between the tip and the sample surface, d_{piezo} is the piezo scanner position in nanometers, d_{def} is the deflection signal of the cantilever in volts, and m_{cl} is the slope

* Phone: 0049-6131-39-2447. Fax: 0049-6131-39-2970. E-mail: astridd@wintermute.chemie.uni-mainz.de.

S1089-5647(98)01396-0 CCC: $15.00
Published on Web 09/11/1998

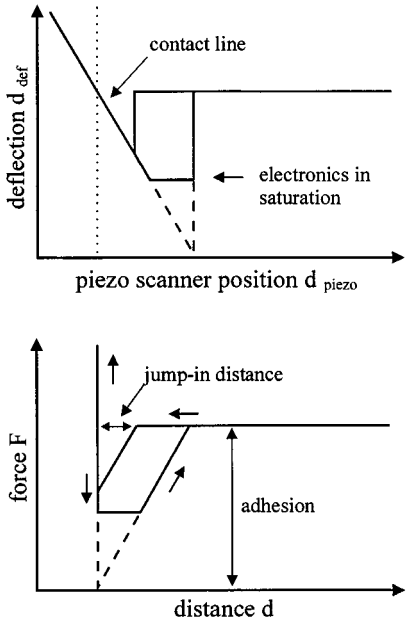

Figure 1. Calibration of force curves. The force was obtained by multiplying the cantilever deflection d_{def}/m_{cl} with the spring constant K. To convert the scanner position d_{piezo} into the distance d, the term d_{def}/m_{cl} had to be subtracted. m_{cl} is the slope of the contact line. The dashed lines show the assumed behavior of the force curves in the electronics-limited part.

of the linear, retracting part of the contact line in volts per nanometer (Figure 1). The term d_{def}/m_{cl} is the deflection of the cantilever in nanometers. It corrects for the cantilever bending. The force is $F = Kd_{def}/m_{cl}$. K denotes the spring constant. The point of zero distance was determined from the linear, retracting part of the contact line.

The time resolution of the electronics was fast compared to the resonance frequency of the cantilever. Therefore it did not affect our measurements. The z-component of the piezo scanner was calibrated at room temperature as described in ref 45. It changes by roughly 0.5%/°C.

Force curves were not averaged, because the signal-to-noise ratio was quite high. In addition, averaging can cause significant artifacts when the cantilever bending or the sample height is even slightly drifting. The maximal applied force of 20 nN varied within ±10%. Since the contact lines went into saturation at about 9 nN, the maximal applied force was estimated by extrapolation.

Ice samples were prepared by freezing Millipore water with a conductivity of 0.06 μS/cm on a freshly cleaved mica sheet. Since the ice layers were only approximately 0.5 mm thick, they froze within seconds. A new sample was used for each experiment. The experiments were partly done in the cold chamber of the DLR (Deutsches Zentrum für Luft- und Raumfahrt e.V.) in Cologne and partly in a freezer of 300 L volume which could be cooled to −40 °C. To increase the thermal capacity, we filled the freezer with cans containing 50 L of ice. The air humidity determined with an electronic thermo-hygrometer was 80%. It is possible that the ice was slightly sublimated away, but we cannot distinguish between sublimation and drift of the cantilever. In any case the sublimation or drift was on the order of 1 nm/s. The temperature was measured by a thermocouple device (accuracy 0.5 °C absolute and 2% relative), which was positioned directly above the ice. The temperature difference between the position of the thermocouple and the ice surface was less than 0.5 °C.

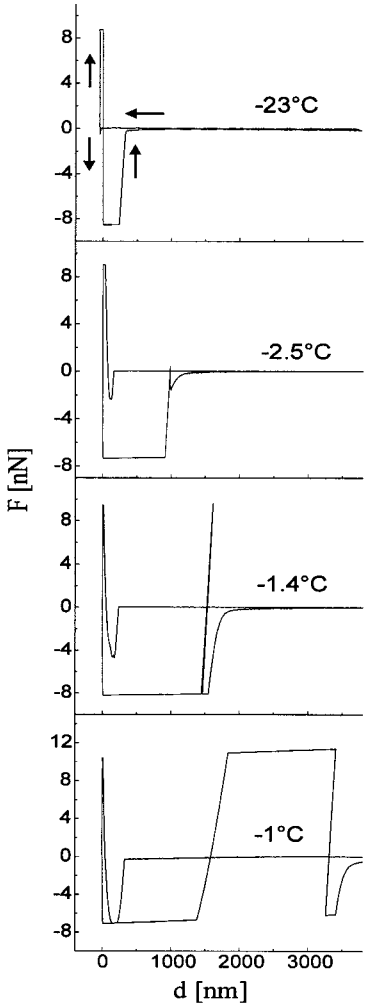

Figure 2. Force curves measured at different temperatures at a frequency of 10 Hz. The saturated part of the contact lines that was used to determine the maximal applied force is not shown in these force curves.

3. Results and Discussion

Figure 2 shows force-versus-distance curves (called force curves) measured at different temperatures and a frequency (measured force curves per second) of 10 Hz. The distance between the ice surface and the tip is plotted versus the force on the tip. While the tip is far away from the ice, the force on the tip is zero. At a certain distance the tip jumps into contact with the surface. We call that distance the jump-in distance. When the tip is in contact and the sample is perfectly rigid, one expects a straight force-versus-position curve and hence a vertical line in the force-versus-distance curve since the position of the tip with respect to the sample surface does not change anymore. Any increase of the force should not change the tip position. Measured force curves, however, deviated significantly from a straight line. This is obvious at −2.5 and −1.4 °C. An analysis of force curves measured at lower temperatures also revealed a deviation of the contact part from a straight line. Such a deviation shows that the tip penetrated the ice. The degree of penetration increased roughly linearly with increasing temperature.

When retracting the tip again, it had to be pulled off the ice surface with a relatively strong force. We call this force the adhesion force. The jump-in distance and the adhesion force increased with increasing temperature. In most cases the adhesion was so strong that the electronic amplifiers and hence

the force signal went into saturation. Then adhesion was measured by multiplying the jump-out distance with the spring constant of the cantilever. This neglects a possible neck formation in the attractive regime. The assumed behavior in the electronics-limited part of the force curves is shown as dashed lines in Figure 1. Several force curves show some curvature after jump-out. We are not sure what causes this curvature. Probably it is caused by relaxation of the cantilever. To avoid an influence on the adhesion force, we have determined the jump-out distance by extrapolating the linear part of the jump-out line to zero force.

At temperatures above −1.4 °C no adhesion measurements were possible because the force curves were distorted, as one can see in the last force curve of Figure 2. A possible explanation for this distortion is that the tip penetrated the ice so deeply that a lateral movement during withdrawing was hindered. As soon as the tip is in contact, it has to move laterally over the surface, since the cantilever length is constant, but the angle between cantilever and sample surface decreases. This lateral movement continues until the piezo scanner stops and changes its direction. Then the angle increases, which leads to a lateral movement in the opposite direction. Friction during this lateral movement bows the cantilever. With the optical lever detection system the bow causes the light beam to be offset. This leads to a hysteresis in the contact region of the force curve. On a homogeneous, smooth surface a parallel displacement of the approaching part with respect to the retracting part of the force curve is observed[46] (Figure 2, top at −23 °C). If the tip cannot slide freely over the surface, it has to tilt, which leads to a distorted position signal.

With respect to the properties of an ice surface three effects are especially significant. The first one is the jump-in during the approach. It is characterized by the jump-in distance, and it contains information about the thickness of the liquidlike layer. The second effect is the deviation of the contact line from a straight line. It indicates a penetration of the tip into the ice. The third effect is adhesion. The adhesion force is probably determined by the thickness of the liquidlike layer and by the distance the tip penetrates the ice. These three effects were studied in more detail.

Thickness of the Liquidlike Layer. Figure 3a shows the measured jump-in distances versus temperature at a frequency of 10 Hz. Between −24 and −10 °C the jump-in distance remained almost constant at a value of 10−16 nm. Above −10 °C it increased to a maximum of about 70 nm at −0.7 °C. These values are significantly larger than the mean value of the jump-in distance of about 3.5 nm at −10.7 °C as it was measured by Petrenko,[16] although in two cases he found similar jump-in distances of 13 and 16 nm which agree with our measurements.

The jump-in is probably caused by the capillary force. As soon as the tip touches the surface of the liquidlike layer, the tip surface is wetted by water. The bending of the water surface at the meniscus causes a negative Laplace pressure which pulls the tip onto the ice surface. In addition, the surface tension of water causes a downward force.[47]

The dependence of the jump-in distance on frequency at −19 °C is shown in Figure 4a. Between 2 and 32 Hz the jump-in distance was constant. For frequencies smaller than 2 Hz it increased. Force curves at frequencies smaller than 2 Hz had a significantly different shape (Figure 5). Up to four jump-ins were recognizable in force curves measured at 0.1 Hz. Even though the exact forms of these force curves were hardly reproducible, at least two jump-ins were usually visible. To determine the frequency dependence of the jump-in distance,

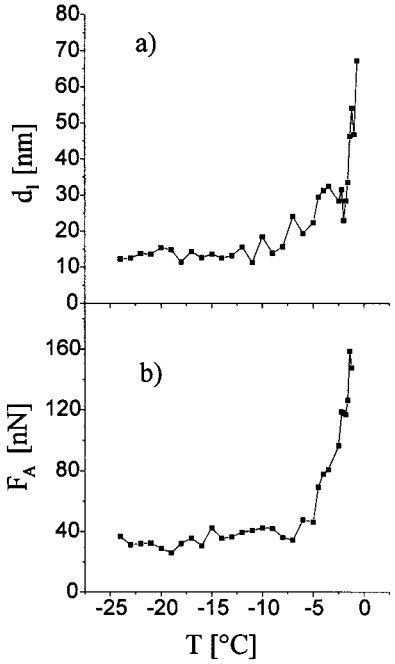

Figure 3. Upper limit of the thickness of the liquidlike layer on ice d_l (top) and the adhesion force F_A (bottom) versus temperature at a frequency of 10 Hz. Both are increasing with temperature. The maximal applied force of 20 nN was kept constant within ±10%.

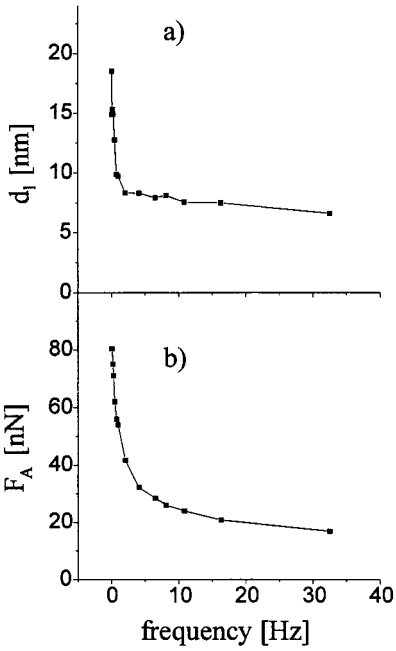

Figure 4. Upper limit of the thickness of the liquidlike layer on ice d_l (top) and the adhesion force F_A (bottom) versus frequency (measured force curves per second). The temperature was −19 °C. Both quantities are decreasing with increasing frequency.

we used only force curves with not more than two jump-ins. The jump-in distance was determined from the first jump-in.

This behavior cannot be explained by a lateral stick−slip motion of the tip over the surface, because at the first jump-in the tip is too far away from the surface. In addition, the apparent force curve would show a continuously increasing attractive force (stick) followed by a "jump-up" from the surface (slip). This was not observed. A possible explanation is that a solid ice bridge was formed between tip and sample during approach, caused by capillary condensation to the liquid or solid phase. Such a bridge could drastically change the shape of force curves.

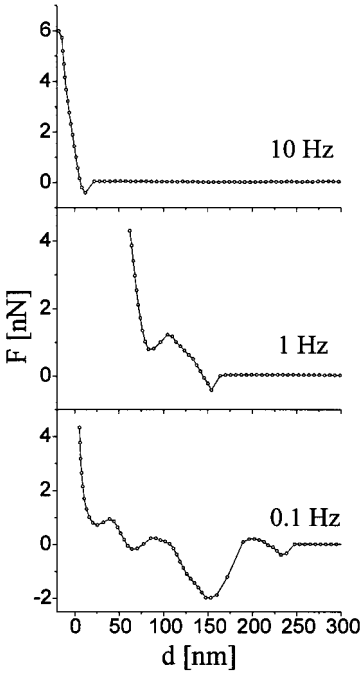

Figure 5. Force curves measured at different frequencies at a temperature of −17 °C. Only the approaching part is shown. The additional features at 1 and 0.1 Hz may be due to capillary condensation.

The jump-in distance is an upper limit of the thickness of the liquidlike layer on ice. Capillary condensation might play a role even at frequencies above 2 Hz. However, we do not think it had a significant influence. The sharp increase of the jump-in distance at frequencies below 2 Hz indicates that the process is strongly time dependent and is probably virtually absent at high frequencies. Still, we cannot principally exclude a significant contribution even at high frequencies.

In addition, the van der Waals attraction needs to be considered. For a spherical tip of radius R interacting with a plane the van der Waals force can be approximated by

$$F_{\mathrm{vdW}} = -\frac{HR}{6d^2}$$

The negative sign indicates that the force is attractive. H is the Hamaker constant; for solids or liquids interacting across vacuum or gas it is on the order of $H \approx 5 \times 10^{-20}$ J. Any attractive force leads to a jump-in of the tip when the gradient of the attraction exceeds the spring constant of the cantilever. With a spring constant of 0.1 N/m and a typical radius of 10 nm the van der Waals force should lead to a jump-in at a distance of ≈1.2 nm. Using a spring constant of 0.23 N/m and a tip radius of 50 nm leads to almost the same result (0.9 nm). In addition, the liquidlike layer might be deformed and bulge up toward the tip surface. This could lead to a jump-in at even larger distances.

Penetration of the Tip into the Ice Surface. When the tip was in contact with the surface, the force curves deviated markedly from a straight line and looked similar to force curves obtained on highly deformable substrates (Figure 6). This shows that the ice surface beneath the liquidlike layer was not rigid and that the tip penetrated into the ice.

To examine the temperature dependence of this penetration, we determined the force F_p that was necessary to press the tip a certain distance (5 nm) into the ice. We used the same force curves that we measured to determine the jump-in distance and the adhesion force. F_p decreased roughly linearly with increasing temperature (Figure 7). Even at the lowest temperatures the ice surface was deformable, but below −19 °C F_p could not be determined because the maximal measured penetration depth was less than 5 nm, which indicates a discontinuous change of F_p. At temperatures above −4 °C F_p became negative. This was probably due to the capillary force of the liquidlike layer; the effective force is the sum of the capillary force plus the externally applied force.

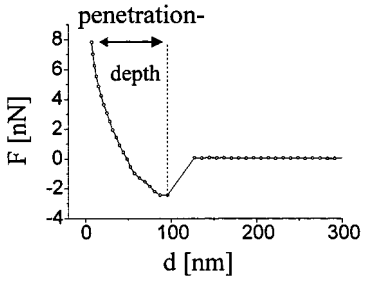

Figure 6. Force curve measured at −3.5 °C with a frequency of 10 Hz (circles). The dashed line represents a force curve of an infintely rigid surface. The difference between the measured and the theoretical line indicates that the tip penetrated the ice.

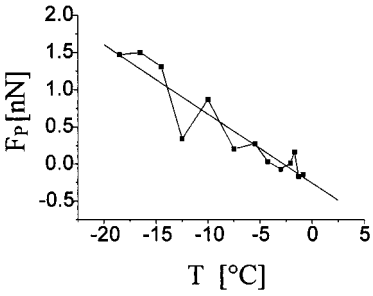

Figure 7. Force that is needed to press the tip 5 nm into the ice surface, F_p, versus temperature at a frequency of 10 Hz. F_p decreases roughly linearly with increasing temperature.

A simple calculation proves that this penetration cannot be due to pressure melting: If the penetration would be completely caused by pressure melting, we could use the F_p -versus-temperature curve to determine the tip radius. If we assume a parabolic tip, the relation between F_p and the melting pressure of ice P_S is

$$F_p = 2\pi z R P_S$$

R is the tip radius of curvature, and z, the penetration depth (5 nm). For simplicity we used a linear dependence between the melting pressure and the temperature: $P_S \approx (-96\ \mathrm{bar/°C})T$. Using a linear approximation, the actual melting pressure is slightly underestimated, and in the following argument we are on the safe side. Now we can determine the tip radius from the slope of F_p and get $R < 0.5$ nm compared to the real radius of approximately 10 nm. Therefore we conclude that the significant part of tip penetration is not due to pressure melting. The discontinuous change of F_p below −19 °C possibly indicates that pressure melting cannot be excluded completely but a small contribution of pressure melting to the penetration of the tip into the ice is not relevant for the following interpretation of our results. In addition, Petrenko[16] found that pressure melting has never occurred in his AFM experiments at $T \leq -1.5$ °C, which is due to the plasticity of ice as measured in ref 48.

The penetration of the tip into the ice can be interpreted in two ways:

(1) A "soft ice layer" exists between the liquidlike layer and the bulk ice. If such a soft ice layer exists, the AFM

measurements indicate a clear phase boundary toward the liquidlike layer since the force curves show a sharp change. The jump-in through the liquid layer is very fast and only limited by the resonance frequency of the cantilever of 20−40 kHz. The penetration into the ice is at least 2 orders of magnitude slower. Above −1 °C the boundary became smudged.

(2) The presence of the solid tip surface causes the ice surface to change its mechanical properties. In the following text we call it interfacial premelting. This process has to be clearly distinguished from surface premelting. (Surface premelting is responsible for the liquidlike layer, which is characterized by the jump-in distance.)[20,49,50] Interfacial premelting could be caused by surface forces between the silicon nitride tip and the ice.

We favor the second explanation of interfacial premelting. Earlier experiments[51−53] point in the same direction. In particular wire regelation experiments support this view. A loaded wire moves through a block of ice even at temperatures significantly below the freezing point.[54−57] A reduction of the chemical potential of liquid water with respect to ice close to a solid surface has been postulated to explain this observation.[56] Such a difference in the chemical potential could be caused by van der Waals forces.[49] In addition, Furukawa and Ishikawa[58] and Beaglehole and Wilson[59] have investigated the ice/glass interface using ellipsometry. Furukawa and Ishikawa found a layer with a refractive index close to that of bulk water (liquidlike layer) above −1 °C. The thickness of this layer increased rapidly as the temperature approached the melting point of ice. Beaglehole and Wilson found no liquid film between ice and smooth glass, but between ice and roughened glass they found films above −5 °C.

The conditions under which a variety of ice/substrate interfaces undergo complete interfacial melting have been investigated theoretically by Wilen et al.[49] Using DLP theory,[60] they found that, for some substrates, for example tungsten, interfacial melting did not occur. In the case of silicon they calculated layer thicknesses on the order of several 0.1 nm to about 20 nm in the temperature range of ≈ -10 to -10^{-5} °C.

Strausky et al.[61] proposed that the heat of friction is not used to melt the ice below the slider but to increase the temperature of an ice layer with a depth of about 100 μm. In this case both interfacial premelting and the permanent existence of a soft ice layer could help to explain the low friction on ice. Especially interfacial premelting could be a significant factor in explaining the existence of the lubricating liquid layer between the solid and ice.

Adhesion Force. The adhesion force showed almost the same temperature dependence as the jump-in distance (Figure 3b). Between −24 and about −5 °C there was almost no change in adhesion. From −5 to −1 °C the adhesion force increased by a factor of about 3.

The adhesion force decreased with increasing frequency (Figure 4b). This monotonic decrease was less steep than for the jump-in distance. The dependence of the adhesion force on frequency can be explained by a deeper penetration of the tip into the ice at lower frequencies. The deeper the tip penetrates into the ice, the bigger the contact area and the higher the adhesion force.

Petrenko[16] wrote, "The general impression that one receives in studying the surface of ice on a microscopic scale and at temperatures above −20 °C is that the surface is very mobile, changeable, and tricky." We can only agree with that. We measured the temperature dependence of force curves three times on different samples with different tips. The general shape

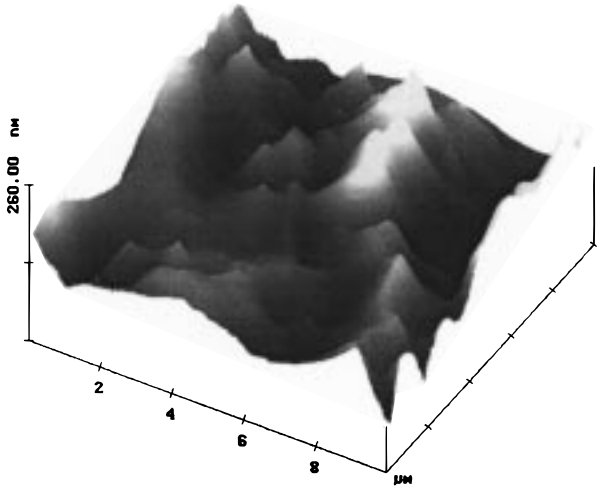

Figure 8. Topographic image of ice measured at −20 °C in contact mode.

of the force curves and the dependence of the jump-in distances and adhesion forces on frequency and temperature were always the same. However, the exact values differed by a factor of about 2. Changing the location of the tip on the ice sample also changed force curves, although not that strongly. When we measured force curves at the same temperature, within a short time (several minutes) and without changing the position, we found deviations of the jump-in distances smaller than 30% and of the adhesion forces smaller than 5%.

In addition to taking force curves, we imaged the surface of ice at −20 °C in contact mode (Figure 8). Images taken in tapping mode looked similar. Apparently the ice surface was not a smooth plane but relatively rough. Typical peak-to-valley distances were on the order of 100 nm. The origin of this roughness is still unclear. This might be a problem when determining the thickness of the liquidlike layer. Different layer thicknesses may develop on top of "icebergs" and in "valleys" driven by the surface tension. Hence, the thickness might be higher in valleys than on top of icebergs. In addition, the valleys can be filled with water by capillary condensation.[62] This might explain the different jump-in distances measured at different positions. Different thicknesses of the liquidlike layer also influence the measurement of adhesion and friction.

Friction Measurements. When a line scan is performed with the scan direction being perpendicular to the cantilever axis, the tip will be tilted laterally due to the friction force between tip and sample. This causes a lateral deflection of the reflected laser beam which is measured using a segmented photodiode. This constant lateral deflection during a line scan (trace) with constant speed yields a detector output voltage U_{fr}^{trace}. Reversing the scan direction (retrace) induces a tilt to the opposite side. The difference between the two signals, $\Delta U_{fr} = U_{fr}^{retrace} - U_{fr}^{trace}$, is proportional to the friction force (Figure 9). We measured friction curves with a maximum scan size, d_{scan}, of 500 nm. To determine ΔU_{fr}, the trace and retrace were fitted with a line fit. At the beginning of each scan one can see the relaxation of the tip to its equilibrium tilt angle. Therefore we fitted only the last 300 nm (the flat part of the friction curves). As difference signal ΔU_{fr}, we took the difference in the middle of the scan.

While taking friction curves, the tip was moving over the surface perpendicular to the scan direction. Therefore the friction curves were all measured at different locations. Imaging the surface afterward did not reveal surface damages. In addition, we have imaged the surface after measuring friction

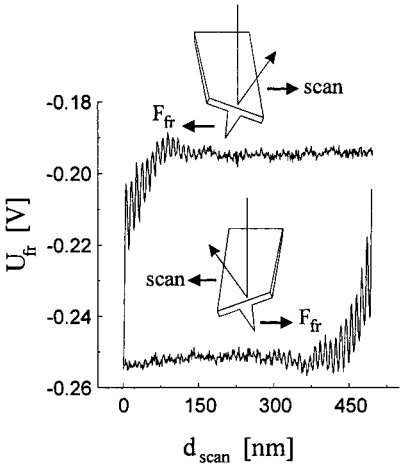

Figure 9. Friction curve measured at 30 Hz at −25.5 °C.

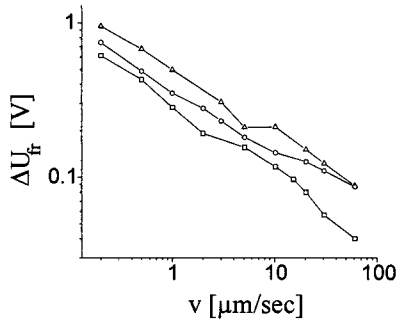

Figure 10. Friction as a function of velocity measured at temperatures of −22 (triangles), −24.5 (circles), and −25.5 °C (squares). ΔU_{fr} is directly proportional to the friction force. The applied normal force was 5 nN.

curves at only one location for about 10 min. In this case the tip furrowed visibly through the ice. These measurements were not further considered.

Friction was measured as a function of velocity in the range of 0.2−60 μm/s with a normal force of 5 nN. The normal force was checked for constancy before and after the experiment. It varied within 15%. Friction increased with decreasing velocity (Figure 10). At a sliding velocity of 0.2 μm/s friction was more than 1 order of magnitude higher than at 60 μm/s. This general dependence of friction on sliding velocities was also observed on a macroscopic level.[38,48]

Measuring friction was sometimes difficult due to the inhomogeneity of the ice surface (Figure 11). However, changes in friction at different places on the surface were small (≈30−40%) compared to changes at different velocities.

A possible explanation for the dependence of friction on velocity is the penetration of the tip into the ice. The smaller the velocity, the more the tip can penetrate the ice and the higher its resistance to sliding will be. This result can also be transferred to friction between a macroscopic slider and ice, because the interaction between slider and ice is at least partly restricted to microscopic contact areas.

Influence of the Laser Heat. Since the deflection of the AFM tip was detected with a laser beam, we had to make sure that the ice was not melted by the heat of the laser.[63] A sensitive quantity for detecting the melting of ice is the adhesion force. Therefore we measured the adhesion force without filter and with filters that reduced the laser intensity to 25% and 10% in a temperature range between −13 and −1.5 °C. Within the error range we did not see a change in the adhesion force at and below −3 °C. At −1.5 °C we saw that the adhesion force

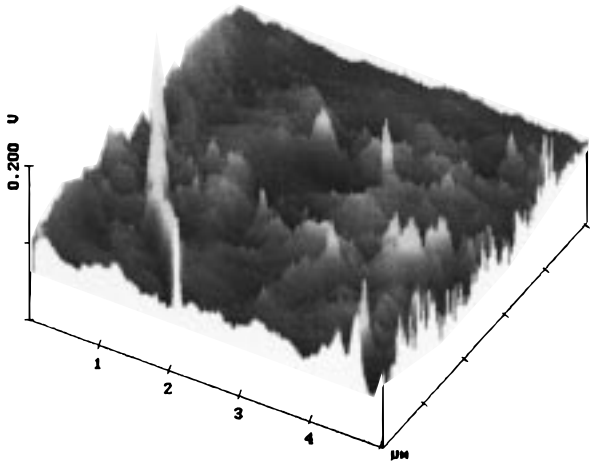

Figure 11. Image of the ice surface taken in friction mode at a temperature of −20 °C.

measured without filter was increased by 30−35% compared to the adhesion force measured with a 10% filter. Above approximately −1.5 °C adhesion measurements were hardly possible (see above). To avoid heating, we used the 10% filter for all experiments. Even with that filter it is possible that our results are slightly influenced by the laser, but that influence is not more than several percent compared to changes of several hundred percent in the adhesion force caused by temperature changes.

4. Conclusion

The surface of ice can be investigated with an atomic force microscope. Reducing the laser intensity with different optical filters did not influence the adhesion force significantly.

An upper limit of the thickness of the liquidlike layer on ice was measured. It increased with increasing temperature. The influence of van der Waals attraction and capillary condensation on the jump-in distance has to be examined in more detail to determine its thickness precisely.

The tip penetrated into the ice. The force that is needed to press the tip a certain distance into the ice surface decreased roughly linearly with increasing temperature. This indicates that either a soft ice layer exists below the liquidlike layer or the presence of the solid tip surface decreases the stiffness of the ice surface. Such an interfacial premelting might also be responsible for the lubricating liquid layer which reduces friction. Friction increased with decreasing sliding velocity.

Acknowledgment. We thank Prof. Dr. D. Möhlmann from the DLR (German Aerospace Center, Institute of Space Simulation, Cologne) for putting the cold chamber at our disposal for 2 weeks. Thanks to Markus Preuss for his help in determining the spring constants. The project was partly supported by the DFG (A.D.).

References and Notes

(1) Clary, D. C. *Science* **1996**, *271*, 1509.
(2) Gertner, B. J.; Hynes, J. T. *Science* **1996**, *271*, 1563.
(3) Molina, M. J.; Tso, T.-L.; Molina, L. T.; Wang, F. C. J. *Science* **1987**, *238*, 1253.
(4) Vlachy, V.; Haymet, A. D. J.; *J. Chem. Phys.* **1986**, *74*, 2559.
(5) Elbaum, M.; Lipson, S. G.; Dash, J. G. *J. Cryst. Growth* **1993**, *129*, 491.
(6) Furukawa, Y.; Kuroda, T.; Yamamoto, M. *J. Cryst. Growth* **1987**, *82*, 665.
(7) Furukawa, Y.; Yamamoto, M.; Kuroda, T. *J. Phys., Colloq. C1* **1987**, *48*, 495.
(8) Beaglehole, D.; Nason, D. *Surf. Sci.* **1980**, *96*, 357.

(9) Kouchi, A.; Furukawa, Y.; Kuroda, T. *J. Phys. Colloq.* **1987**, *48*, 675.
(10) Dosch, H.; Lied, A.; Bilgram, J. H. *Phys. Rev. Lett.* **1994**, *72*, 3534.
(11) Golecki, I.; Jaccard, C. *Phys. Lett. A* **1977**, *63*, 374.
(12) Ishizaki, T.; Maruyama, M.; Furukawa, Y.; Dash, J. G. *J. Cryst. Growth* **1996**, *163*, 455.
(13) Mizuno, Y.; Hanafusa, N. *J. Phys., Colloq. C1* **1987**, *48*, 511.
(14) Morgenstern, M.; Müller, J.; Michely, T.; Comsa, G. *Z. Phys. Chem.* **1997**, *198*, 43.
(15) Nickolayev, O.; Petrenko, V. F. *Mater. Res. Soc. Symp. Proc.* **1995**, *355*, 221.
(16) Petrenko, V. F. *J. Phys. Chem. B* **1997**, *101*, 6276.
(17) Slaughterbeck, C. R.; Kukes, E. W.; Pittenger, B.; Cook, D. J.; Eden, V. L.; Williams, P. C.; Fain, S. C. *J. Vac. Sci. Technol. A* **1996**, *14*, 1213.
(18) Pittenger, B.; Cook, D. J.; Slaughterbeck, C. R.; Fain, S. C. *J. Vac. Sci. Technol. A* **1998**, *16*, 1832.
(19) Petrenko, V. F. CRREL Special Report 94-22; Cold Regions Research and Engineering Laboratory, Hanover, NH, 1994.
(20) Dash, J. G.; Haiying, F.; Wettlaufer, J. S. *Rep. Prog. Phys.* **1995**, *58*, 115.
(21) Jellinek, H. H. G. *J. Colloid Interface Sci.* **1967**, *25*, 192.
(22) Fletcher, N. H. *Philos. Mag.* **1968**, *18*, 1287.
(23) Elbaum, M.; Schick, M. *Phys. Rev. Lett.* **1991**, *66*, 1713.
(24) Materer, N.; Starke, U.; Barbieri, A.; Van Hove, M. A.; Somorjai, G. A.; Kroes, G.-J.; Minot, C. *Surf. Sci.* **1997**, *381*, 190.
(25) Furukawa, Y. *Chem. unserer Z.* **1997**, *2*, 58.
(26) Makkonen, L. *J. Phys. Chem. B* **1997**, *101*, 6196.
(27) Oksanen, P.; Keinonen, J. *Wear* **1982**, *78*, 315.
(28) Slotfeldt-Ellingsen, D.; Torgersen, L. *J. Phys. D: Appl. Phys.* **1983**, *16*, 1715.
(29) Balakin, V. A.; Pereverzeva, O. V. *Sov. J. Frict. Wear* **1991**, *12* (3), 132.
(30) Colbeck, S. C. CRREL Monograph 92-2; Cold Regions Research and Engineering Laboratory, Hanover, NH, 1992.
(31) Fowler, A. J.; Bejan, A. *Int. J. Heat Mass Transfer* **1993**, *36* (5), 1171.
(32) Petrenko, V. F.; Colbeck, S. C. *J. Appl. Phys.* **1995**, *77* (9), 4518.
(33) Rist, M. A. *J. Phys. Chem. B* **1997**, *101*, 6263.
(34) Reynolds, O. *Papers on Mechanical and Physical Subjects*; Cambridge University Press: Cambridge, U.K., 1901; Vol. 2, p 734.
(35) Colbeck, S. C.; Najarian, I.; Smith, H. B. *Am. J. Phys.* **1997**, *65* (6), 488.
(36) Bowden, F. P.; Hughes, T. P. *Proc. R. Soc. London, A* **1939**, *172*, 280.
(37) Bowden, F. P. *Proc. R. Soc. London* **1953**, *217*, 462.
(38) Evans, D. C. B.; Nye, J. F.; Cheeseman, K. J. *Proc. R. Soc. London, A* **1976**, *347*, 493.
(39) Colbeck, S. C. *J. Sports Sci.* **1994**, *12*, 285.
(40) Binnig, G.; Quate, C. F.; Gerber, C. *Phys. Rev. Lett.* **1986**, *56*, 930.
(41) Siedle, P.; Butt, H.-J.; Bamberg, E.; Wang, D. N.; Kuehlbrandt, W.; Zach, J.; Haider, M. *Int. Phys. Conf. Ser.* **1992**, *130*, 361.
(42) Derjaguin, B. *Kolloid-Z.* **1934**, *69*, 155.
(43) Hutter, J. L.; Bechhoefer, J. *Rev. Sci. Instrum.* **1993**, *64*, 1868.
(44) Markus Preuss, M.; Butt, H.-J. Submitted for publication in *Int. J. Miner. Process.* **1998**.
(45) Jaschke, M.; Butt, H.-J. *Rev. Sci. Instrum.* **1995**, *66*, 1258.
(46) Hoh, J. H.; Engel, A. *Langmuir* **1993**, *9*, 3310.
(47) Israelachvilli, J. *Intermolecular and Surface Forces*; Academic Press: New York, 1992; p 330.
(48) Barnes, P.; Tabor, D.; Walker, F. R. S.; Walker, J. C. F. *Proc. R. Soc. London, A* **1971**, *334*, 127.
(49) Wilen, L. A.; Wettlaufer, J. S.; Elbaum, M.; Schick, M. *Phys. Rev. B* **1995**, *52* (16), 12426.
(50) Wettlaufer, J. S.; Worster, M. G.; Wilen, L. A.; Dash, J. G. *Phys. Rev. Lett.* **1996**, *76* (19), 3602.
(51) Anderson, D. M. *J. Colloid Interface Sci.* **1967**, *25*, 174.
(52) Römkens, M. J. M.; Miller, R. D. *J. Colloid Interface Sci.* **1973**, *42 (1)*, 103.
(53) Mantovani, S.; Valeri, S.; Loria, A.; del Pennino, U. *J. Chem. Phys.* **1980**, *72* (2), 1077.
(54) Telford, J. W.; Turner, J. S. *Philos. Mag.* **1963**, *8*, 527.
(55) Drake, L. D.; Shreve, R. L. *Proc. R. Soc. London, A* **1973**, *332*, 51.
(56) Gilpin, R. R. *J. Colloid Interface Sci.* **1978**, *68* (2), 235.
(57) Gilpin, R. R. *J. Colloid Interface Sci.* **1980**, *77* (2), 435.
(58) Furukawa, Y.; Ishikawa, I. *J. Cryst. Growth* **1993**, *128*, 1137.
(59) Beaglehole, D.; Wilson, P. *J. Phys. Chem.* **1994**, *98*, 8096.
(60) Dzyaloshinskii, I. E.; Lifshitz, E. M.; Pitaevskii, L. P. *Adv. Phys.* **1961**, *10*, 165.
(61) Strausky, H.; Krenn, J. R.; Leitner, A.; Aussenegg, F. R. *Appl. Phys. B* **1998**, *66*, 599.
(62) Celestini, F. *Phys. Lett. A* **1997**, *228*, 84.
(63) Eastman, T.; Zhu, D. *J. Colloid Interface Sci.* **1995**, *172*, 297.